Phagraphene: A Low-Energy Graphene Allotrope Composed of 5−6−7 Carbon Rings with Distorted Dirac Cones

Zhenhai Wang,[*,†,‡] Xiang-Feng Zhou,[‡,§] Xiaoming Zhang,[∥] Qiang Zhu,[‡] Huafeng Dong,[‡] Mingwen Zhao,[*,∥] and Artem R. Oganov[*,‡,⊥,#,∇]

[†]Peter Grünberg Research Center, Nanjing University of Posts and Telecommunications, Nanjing, Jiangsu 210003, China

[‡]Department of Geosciences, Center for Materials by Design, and Institute for Advanced Computational Science, Stony Brook University, Stony Brook, New York 11794, United States

[§]School of Physics and Key Laboratory of Weak-Light Nonlinear Photonics, Nankai University, Tianjin 300071, China

[∥]School of Physics and State Key Laboratory of Crystal Materials, Shandong University, Jinan, Shandong 250100, China

[⊥]Skolkovo Institute of Science and Technology, Skolkovo Innovation Center, Bldg.3, Moscow 143026, Russia

[#]Moscow Institute of Physics and Technology, 9 Institutskiy Lane, Dolgoprudny City, Moscow Region 141700, Russia

[∇]School of Materials Science, Northwestern Polytechnical University, Xi'an 710072, China

ⓢ Supporting Information

ABSTRACT: Using systematic evolutionary structure searching we propose a new carbon allotrope, phagraphene [**fæ'græfi:n**], standing for **p**enta-**h**exa-hept**a**-graphene, because the structure is composed of 5-6-7 carbon rings. This two-dimensional (2D) carbon structure is lower in energy than most of the predicted 2D carbon allotropes due to its sp²-binding features and density of atomic packing comparable to graphene. More interestingly, the electronic structure of phagraphene has distorted Dirac cones. The direction-dependent cones are further proved to be robust against external strain with tunable Fermi velocities.

KEYWORDS: *Two-dimensional carbon allotrope, distorted Dirac cones, evolutionary algorithm, density functional theory, tight binding, energy band inversion*
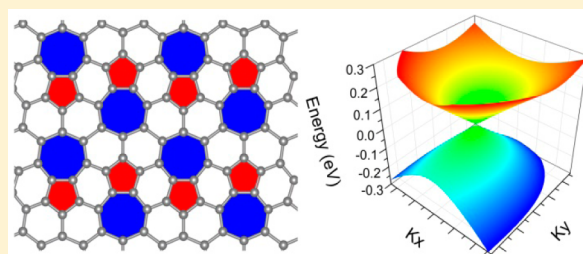
Graphene, as the most stable two-dimensional (2D) form of carbon, exhibits a number of unusual electronic and spintronic properties,[1] such as high carrier mobility[2] and quantum Hall effect.[3,4] Its honeycomb lattice, which has perfect hexagonal symmetry, plays a crucial role in the formation of the Dirac cones with linear dispersion. Successful preparation of graphene in 2004[5] has inspired further search for other 2D Dirac materials. Among the predicted 2D Driac materials[6] are silicene,[7] germanene,[7] silicon germanide monolayer,[8] graphynes,[9,10] *Pmmn* boron,[11] *m*-TiB₂,[12] so-MoS₂,[13] and so forth, while only Dirac cones in graphene have been actually confirmed experimentally.[14] The stable and robust 2D carbon backbone motivate the searches for other Dirac carbon allotropes.

Graphynes, composed of sp and sp² hybridized atoms, were first proposed in 1987[15] with various structures and high thermal stability. These graphynes can be metallic, semimetallic, or semiconducting.[16,17] Up to 2012, Malko et al.[9] reported that α-, β-, and 6,6,12-graphyne could have Dirac cones. Huang et al. have tried to derive a criterion to explain the physical origin of the existence or absence of Dirac cones in graphynes in which they successfully predicted two other graphynes with Dirac cones, 14,14,14-graphyne and 14,14,18-graphyne.[18] After

that, δ-graphyne was proposed as another Dirac carbon allotrope, which was demonstrated to be a carbon topological insulator superior to graphene.[10] For all these graphynes with Dirac cones, α-, β-, and δ-graphynes exhibit hexagonal symmetry, while 6,6,12-, 14,14,14-, and 14,14,18-graphynes have rectangular lattices, which suggests that the hexagonal symmetry is not a necessary precondition for the presence of Dirac cones.[19]

However, the sp-hybridization of carbon atoms involved in these graphynes is energetically disadvantageous compared with that of sp²- and sp³-carbon atoms. Several carbon allotropes composed of sp²- and sp³-carbon atoms have also been predicted to have Dirac cones. Liu et al. proposed "T-graphene" in 2012, named after a buckled carbon sheet with tetrarings, as a 2D Dirac material.[20] Although it was argued to be metallic in a subsequent work,[21] the Dirac-like fermions and high Fermi velocity predicted in bulked T-graphene open a possibility to find novel 2D Dirac graphene allotropes with multimember rings. In 2014, Xu et al. designed three rectangular allotropes by

reconstructing graphene, named as S-, D-, and E-graphene. These sp^2- and sp^3-carbon networks were predicted to be stable and have Dirac cones.[22] They also demonstrated that the Dirac cone and the carrier linear dispersion are common features of these 2D carbon allotropes.

In this Letter, we predicted a new carbon allotrope, phagraphene, which is composed of 5-6-7 carbon rings. This planar carbon allotrope is energetically comparable to graphene and more favorable than other carbon allotropes proposed in previous works due to its sp^2-hybridization and dense atomic packing. Both density functional theory (DFT) and tight binding (TB) model confirm the distorted Dirac cone in the first Brillioun zone (BZ) for this 2D carbon structure. The direction-dependent Dirac cone is further proved to be robust against external strain and has tunable Fermi velocities.

In present work, systematic 2D structure searches were performed using the ab initio evolutionary algorithm USPEX[11,23−25] with 6, 8, 10, 12, 14, 16, 18, 20, 22, and 24 carbon atoms per unit cell. The initial thickness was set to zero, since sp- and sp^2-carbon allotropes prefer planar structures at ambient pressure. The newly produced structures were all relaxed, and the energies were used for selecting structures as parents for the new generation of structures. Structure relaxations used the projector-augmented-wave method,[26] as implemented in the Vienna ab initio simulation package (VASP).[27,28] The exchange-correlation energy was treated within the generalized gradient approximation (GGA), using the functional of Perdew, Burke, and Ernzerhof (PBE).[29]

For calculations of specific 2D carbon allotropes in VASP, a kinetic energy cutoff of 600 eV was adopted. BZ integrations were carried out using Monkhorst−Pack sampling grids with resolution of $2\pi \times 0.04$ Å^{-1} for structure optimizations. The atomic positions and lattice constants were optimized using the conjugate gradients (CG) scheme until the force components on each atom were less than 0.01 eV/Å. An adequate k-point sampling ($30 \times 30 \times 1$) was employed for charge density distributions and band structure calculations. Phonon calculations by supercell approach as implemented in the PHONON code[30] were used to examine dynamical stability, and first-principles molecular dynamics simulations under constant temperature and volume (NVT) were performed to check thermal stability.

During structure searches, graphene was found to have the lowest energy among all possible 2D structures. We present a typical example (20 atoms/cell) in Figure 1a. Besides graphene, phagraphene and δ-graphyne[10] with a 20-atom primitive cell were generated during this search. As we can see, the energies for graphene, phagraphene, and δ-graphyne are −9.23, −9.03, and −8.49 eV/atom, respectively. With different atom numbers in unit cell, many 2D carbon structures with hybrid sp- and sp^2-carbon atoms were generated in our searches, but these structures usually have higher energies than sp^2-carbon allotropes. For sp^2-carbon structures, many of them are composed of penta-, hexa-, hepta-, and octa- (5-, 6-, 7-, and 8-) carbon rings. Most of the planar carbon allotropes proposed in previous works can be reproduced in our systematic searches. Their energies and planar atomic densities are plotted in Figure 1b. It is noted that Dirac allotropes mostly have much higher energies compared with graphene (denoted as 1), and structures with higher energies usually have lower planar atomic densities. The planar atomic density of phagraphene (denoted as 27) is 0.37 atom/Å^2, slightly smaller than 0.38 atom/Å^2 of graphene. Thanks to this dense packing of sp^2-
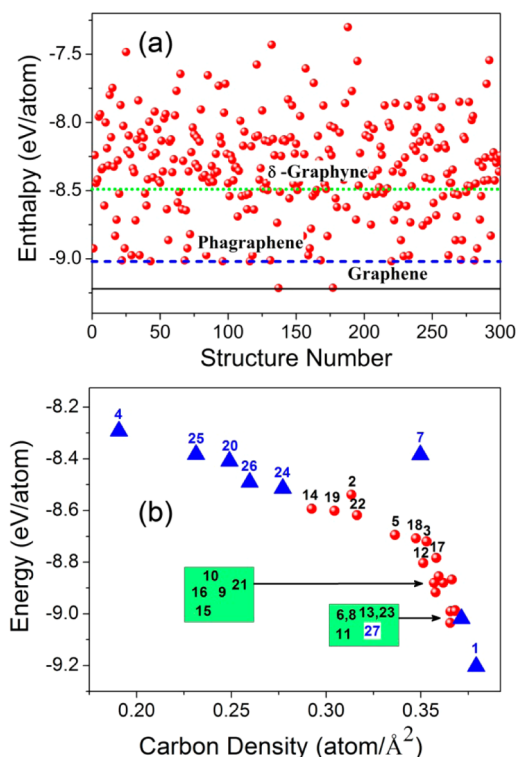

Figure 1. (a) Typical enthalpy evolution for a 20-atom carbon system during an evolutionary structure search; (b) Energies and planar atomic densities for most of 2D carbon allotropes reobtained from our evolutionary structure searches. The codes (from 1 to 27) for these allotropes correspond to the structural serial numbers in Part-III of Supporting Information. Those allotropes with Dirac cones are labeled as blue triangles, and red spheres are for the rest.

carbon atoms, it has lower energy than most of before predicted 2D carbon allotropes.

Figure 2a shows the structure of phagraphene with notable space-inversion symmetry. The structure of phagraphene is composed of 5-6-7 carbon rings. Unlike $P6m$ of graphene and δ-graphyne, the plane group of phagraphene is Pmg. Being surrounded by 6-carbon rings, the pairs with 5- and 7-carbon rings invert to each other and are arranged in a rectangular fashion. Figure 2a also presents the unequivalent carbon atoms (C1−C6) in its unit cell. It is noted that the length of C1−C2 covalent bond is about 1.52 Å, which is longer than that of C2−C3 (1.44 Å), C3−C4 (1.41 Å), C4−C5 (1.43 Å), and C5−C6 (1.40 Å). Moreover, based on our band structure calculations as shown in Figure 2b,c, the valence and conduction energy bands meet at the Fermi level and show the features of a distorted Dirac cone in its first BZ (elaborated in Figure 2b). The density of states (DOS) is zero at the Fermi level, which can further support the presence of the distorted Dirac cone. The Fermi velocities (v_f) of phagraphene in k_x and k_y directions were obtained by fitting these two bands at $k_i = K_i + q$ ($i = x, y$) to the expression $v_f = E(q)/\hbar|q|$, which can be evaluated via the slope of the bands. In the k_x direction, $\partial E/\partial k_x = \pm 26.8$ eVÅ ($v_{fx} = 6.48 \times 10^5$ m/s); in the k_y direction, the slope of the bands equals −25.8 eVÅ ($v_{fy} = 6.24 \times 10^5$ m/s) and 14.2 eVÅ ($v_{fy} = 3.43 \times 10^5$ m/s). These Fermi velocities are comparable with those of other carbon Dirac allotropes predicted in previous works, as listed in Table 1.

In order to explore the origin of the distorted Dirac cone, partial charge density distributions of the two Dirac bands in
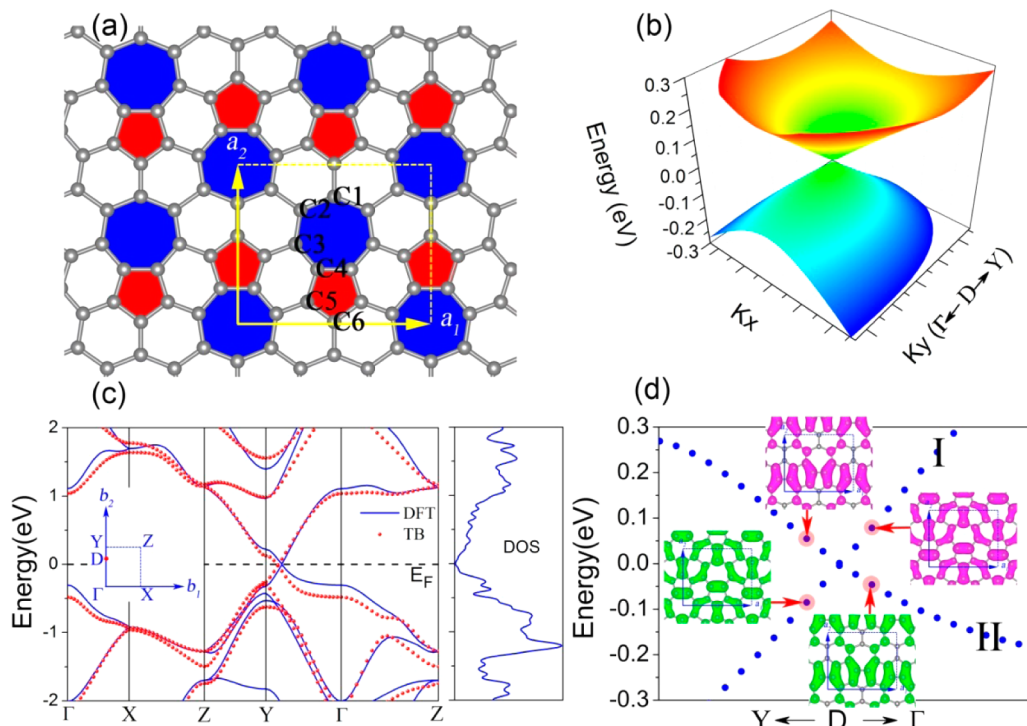
Figure 2. (a) Structure of phagraphene with notable space-inversion symmetry, C1−C6 are unequivalent carbon atoms in its unit cell. (b) Distorted Dirac cone formed by the valence and conduction bands in the vicinity of the Dirac point. (c) Comparison of band structures from DFT (blue line) and TB (red circle) model. The corresponding DOS is zero at the Fermi level. Inserted first BZ with high symmetric k points: Γ (0,0,0), X (0.5,0,0), Z (0.5,0.5,0), Y (0,0,5,0) and Dirac point: D (0, 0.377,0). (d) Charge density distributions near the distorted Dirac cone, both Dirac bands (denoted as I and II) are from p_z orbitals of sp^2-carbon atoms. Fermi level has been set to zero.

Table 1. Calculated Total Energy (E_t) (eV/atom), Planar Carbon Density (D) (atom/Å^2), Plane Group (G), and Fermi Velocities (v_f) (×10^{5}m/s) for Most Carbon Allotropes with Dirac Cones, From GGA-PBE Results

	E_t	D	G	v_f
α-graphyne	−8.30	0.19	$P6m$	6.77
β-graphyne	−8.38	0.23	$P6m$	3.87/4.35/6.77
δ-graphyne	−8.49	0.26	$P6m$	6.96
6,6,12-graphyne	−8.51	0.27	Pmm	5.56/6.04/6.29(Cone I) 1.69/2.18(Cone II)
phagraphene	−9.03	0.37	Pmg	3.43/6.24/6.48
graphene	−9.23	0.38	$P6m$	8.22

proximity of the Fermi level were first investigated, as shown in Figure 2d. It is clear that the occupied states are inversed at the two sides of the Dirac point, which means the energy band inversion. Band-I and band-II, which are mainly contributed by the coupling of p_z orbitals along a_1 and a_2 directions, cross each other and produce the Dirac point. In view of the coupling between p_z orbitals leading to the formation of π-conjugated framework, we adopted a simple tight-binding (TB) Hamiltonian of the π-electrons to describe the electronic band structures in proximity of the Fermi level

$$H = -\sum_{<ij>} t_{ij}c_i^+ c_j + hc \tag{1}$$

where t_{ij} is the hopping energy of an electron between the ith and jth atoms, c_i^+ and c_j are the creation and annihilation operators, respectively. The distance-dependent hoping energy is determined using the formula $t_{ij} = t_0 \exp(q \times (1 - d_{ij}/d_0))$, with $t_0 = 2.70$ eV, $q = 2.20$, and $d_0 = 1.5$ Å. Through

diagonalization of a 20 × 20 matrix in the reciprocal space, the electronic band structures can be obtained, as indicated by the red dashed lines in Figure 2c. Obviously, this simple TB Hamiltonian in eq 1 can reproduce the band structure of phagraphene in the vicinity of the Fermi level given by DFT calculations.

As a matter of fact, most Dirac cones are indeed from the energy band crossing, which can be explained by a simple model: considering a 2-band system, the Hamiltonian can be written as

$$H(k) = \begin{bmatrix} H_{11}(k) - E & H_{12}(k) \\ H_{21}(k) & H_{22}(k) - E \end{bmatrix} \tag{2}$$

The appearance of Dirac cones corresponds to degenerate solutions of this Hamiltonian. In other words, the determinant of $H(k)$ should be equal to zero and the following equations need to be satisfied

$$H_{11}(k) = H_{22}(k); \quad H_{12}(k) = H_{21}(k) = 0 \tag{3}$$

It is intrinsic that these three conditions in eq 3 must be simultaneously fulfilled to have a degeneracy, which is known as the von Neumann-Wigner theorem.[31,32] In most cases, $H_{11}(k)$ = $H_{22}(k)$ can be fulfilled by the space-time inversion symmetries, but the 2D system symmetries cannot guarantee the existence of Dirac cones, because the number of variables (k_x and k_y) is usually less than the number of equations to determine the Dirac points, which gives the reason for the rarity of 2D Dirac materials. As for phagraphene here, band-I and band-II in Figure 2d or Figure 3a can be simply considered as the two bands in above model, only they can appear in the vicinity of the Fermi level and invert to each other, the
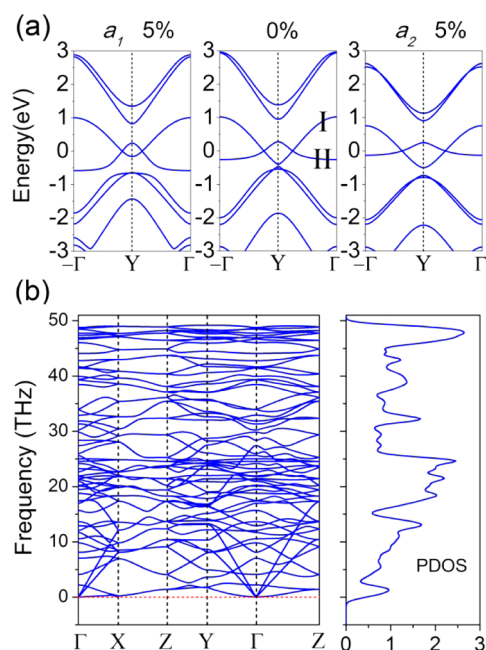
Figure 3. (a) Band structures of phagraphene along $-\Gamma-Y-\Gamma$ line with and without 5% strain along a_1 and a_2 directions, respectively. Fermi level has been set to zero. (b) Phonon dispersion and the PDOS of phagraphene.

distorted Dirac cones are then produced at both sides of space-symmetric and time-invariant k-point Y. Our numerical DFT and TB calculations all reveal that phagraphene happens to fulfill these three conditions simultaneously and presents distorted Dirac cones.

Its direction-dependent character can be further investigated by applying external strain, as shown in Figure 3(a). The cone is stable under 5% strain along a_1 and a_2 directions, respectively. Because of the band symmetry, both position and anisotropy of the Dirac cone can be tuned by external strain. For 5% strain along a_1 direction, the Dirac point moves from (0, 0.377, 0) to (0, 0.417, 0). The corresponding Fermi velocities change from ±26.8 eVÅ to ±23.7 eVÅ in the k_x direction and from $-14.2/25.8$ to $-19.4/28.4$ eVÅ in the k_y direction. Things become different when a 5% strain is added along a_2 direction. Dirac point shifts to (0, 0.313, 0), and the corresponding Fermi velocities become ±28.1 eVÅ in the k_x direction and $-25.4/6.7$ eVÅ in the k_y direction.

In order to examine its dynamic stability, the phonon spectrum and phonon density of states (PDOS) were calculated, as shown in Figure 3b, and no imaginary frequencies were observed. To further examine its thermal stability, a 3×3 supercell was built to perform ab initio molecular dynamics simulations. After being heated at room temperature (300 K) and 1000 K for 3 ps with a time step of 1 fs, no structural changes occurred, only the expected thermal oscillations of the atoms around their equilibrium positions. All these indicate that phagraphene is a potentially synthesizable low-energy carbon allotrope with distorted Dirac cones. Since 5- and 7-carbon ring dislocations and corresponding line defects have been observed in graphene,[33] phagraphene may be realized experimentally in near future.

In summary, systematic ab initio evolutionary structure searches for 2D carbon networks identified a new low-energy 2D form of carbon, composed of 5-6-7 carbon rings and named phagraphene. Thanks to its sp^2-binding features and atomic packing density comparable to that of graphene, this 2D carbon structure with Pmg plane group is lower in energy than most of the predicted 2D carbon allotropes. Both DFT and TB model confirm its distorted Dirac cone. The direction-dependent Dirac cones are further proved to be robust against the external strain with tunable Fermi velocities. This exotic structure is not only promising for fully investigating the massless Dirac fermions in 2D carbon electronic systems but also helpful for understanding the topological and correlated phases in the corresponding photonic artificial lattices.

■ ASSOCIATED CONTENT

Ⓢ Supporting Information

The Supporting Information is available free of charge on the ACS Publications website at DOI: 10.1021/acs.nano-lett.5b02512.

> There are three parts (part I−III): Part I shows large strain effect for the Dirac points. Part II describes the detailed calculations of some phagraphene nanoribbons and nanotubes. Part III lists the details of the 2D carbon allotropes in Figure 1b. (PDF)

■ AUTHOR INFORMATION

Corresponding Authors
*E-mail: wangzh@njupt.edu.cn (Z.W.).
*E-mail: zmw@sdu.edu.cn (M.Z.).
*E-mail: artem.oganov@stonybrook.edu (A.R.O.).
Notes
The authors declare no competing financial interest.

■ ACKNOWLEDGMENTS

■ REFERENCES

(1) Castro Neto, A. H.; Guinea, F.; Peres, N. M. R.; Novoselov, K. S.; Geim, A. K. *Rev. Mod. Phys.* **2009**, *81*, 109−162.
(2) Bolotin, K. I.; Sikes, K. J.; Jiang, Z.; Klima, M.; Fudenberg, G.; Hone, J.; Kim, P.; Stormer, H. L. *Solid State Commun.* **2008**, *146*, 351−355.
(3) Zhang, Y.; Tan, Y.-W.; Stormer, H. L.; Kim, P. *Nature* **2005**, *438*, 201−204.
(4) Bolotin, K. I.; Ghahari, F.; Shulman, M. D.; Stormer, H. L.; Kim, P. *Nature* **2009**, *462*, 196−199.

(5) Novoselov, K. S.; Geim, A. K.; Morozov, S. V.; Jiang, D.; Zhang, Y.; Dubonos, S. V.; Grigorieva, I. V.; Firsov, A. A. *Science* **2004**, *306*, 666−669.

(6) Wang, J.; Deng, S.; Liu, Z.; Liu, Z. *Nati. Sci. Rev.* **2015**, *2* (1), 22−39.

(7) Cahangirov, S.; Topsakal, M.; Aktürk, E.; Şahin, H.; Ciraci, S. *Phys. Rev. Lett.* **2009**, *102*, 236804.

(8) Zhou, H.; Zhao, M.; Zhang, X.; Dong, W.; Wang, X.; Bu, H.; Wang, A. *J. Phys.: Condens. Matter* **2013**, *25*, 395501.

(9) Malko, D.; Neiss, C.; Viñes, F.; Görling, A. *Phys. Rev. Lett.* **2012**, *108*, 086804.

(10) Zhao, M.; Dong, W.; Wang, A. *Sci. Rep.* **2013**, *3*, 3532.

(11) Zhou, X.-F.; Dong, X.; Oganov, A. R.; Zhu, Q.; Tian, Y.; Wang, H.-T. *Phys. Rev. Lett.* **2014**, *112*, 085502.

(12) Zhang, L. Z.; Wang, Z. F.; Du, S. X.; Gao, H. J.; Liu, F. *Phys. Rev. B: Condens. Matter Mater. Phys.* **2014**, *90*, 161402.

(13) Li, W.; Guo, M.; Zhang, G.; Zhang, Y.-W. *Phys. Rev. B: Condens. Matter Mater. Phys.* **2014**, *89*, 205402.

(14) Novoselov, K. S.; Geim, A. K.; Morozov, S. V.; Jiang, D.; Katsnelson, M. I.; Grigorieva, I. V.; Dubonos, S. V.; Firsov, A. A. *Nature* **2005**, *438*, 197−200.

(15) Baughman, R. H.; Eckhardt, H.; Kertesz, M. *J. Chem. Phys.* **1987**, *87*, 6687−6699.

(16) Enyashin, A. N.; Ivanovskii, A. L. *Phys. Status Solidi B* **2011**, *248*, 1879−1883.

(17) Narita, N.; Nagai, S.; Suzuki, S.; Nakao, K. *Phys. Rev. B: Condens. Matter Mater. Phys.* **1998**, *58*, 11009−11014.

(18) Huang, H.; Duan, W.; Liu, Z. *New J. Phys.* **2013**, *15*, 023004.

(19) Liu, Z.; Wang, J.; Li, J. *Phys. Chem. Chem. Phys.* **2013**, *15*, 18855.

(20) Liu, Y.; Wang, G.; Huang, Q.; Guo, L.; Chen, X. *Phys. Rev. Lett.* **2012**, *108*, 225505.

(21) Huang, H.; Li, Y.; Liu, Z.; Wu, J.; Duan, W. *Phys. Rev. Lett.* **2013**, *110*, 029603.

(22) Xu, L.-C.; Wang, R.-Z.; Miao, M.-S.; Wei, X.-L.; Chen, Y.-P.; Yan, H.; Lau, W.-M.; Liu, L.-M.; Ma, Y.-M. *Nanoscale* **2014**, *6*, 1113−1118.

(23) Oganov, A. R.; Glass, C. W. *J. Chem. Phys.* **2006**, *124*, 244704.

(24) Glass, C. W.; Oganov, A. R.; Hansen, N. *Comput. Phys. Commun.* **2006**, *175*, 713−720.

(25) Zhu, Q.; Li, L.; Oganov, A. R.; Allen, P. B. *Phys. Rev. B: Condens. Matter Mater. Phys.* **2013**, *87*, 195317.

(26) Blöchl, P. E. *Phys. Rev. B: Condens. Matter Mater. Phys.* **1994**, *50*, 17953−17979.

(27) Kresse, G.; Furthmuller, J. *Phys. Rev. B: Condens. Matter Mater. Phys.* **1996**, *54*, 11169−11186.

(28) Kresse, G.; Furthmuller, J. *Comput. Mater. Sci.* **1996**, *6*, 15−50.

(29) Perdew, J. P.; Burke, K.; Ernzerhof, M. *Phys. Rev. Lett.* **1996**, *77*, 3865.

(30) Togo, A.; Oba, F.; Tanaka, I. *Phys. Rev. B: Condens. Matter Mater. Phys.* **2008**, *78*, 134106.

(31) Neumann, J. V.; Wigner, E. *Physik Z.* **1929**, *30*, 467.

(32) Landau, L. D.; Lifshitz, L. M. *Quantum Mechanics Non-Relativistic Theory*; Butterworth-Heinemann: Stoneham, MA, 1981.

(33) Yazyev, O. V.; Chen, Y. P. *Nat. Nanotechnol.* **2014**, *9*, 755−767.

E